

## ON-ORBIT VERIFICATION OF GLM NAVIGATION ON GOES-16

Peter J. Isaacson<sup>1</sup>, Alan D. Reth<sup>2,3</sup>, Alexander Krimchansky<sup>2</sup>, Marc D. Rafal<sup>2,4</sup>

<sup>1</sup>The Aerospace Corporation, El Segundo, CA, <sup>2</sup>NASA Goddard Space Flight Center, Greenbelt, MD,

<sup>3</sup>Chesapeake Aerospace LLC, Grasonville, MD, <sup>4</sup>ASRC Federal Technical Services, Beltsville, MD

### Abstract

The GOES-R flight project has developed the Image Navigation and Registration (INR) Performance Assessment Tool Set (IPATS) to perform independent INR evaluations of the optical instruments on the GOES-R series spacecraft. In this paper, we document the development of navigation (NAV) evaluation capabilities within IPATS for the Geostationary Lightning Mapper (GLM). We also discuss the post-processing quality filtering developed for GLM NAV, and present example results for several GLM datasets. Initial results suggest that GOES-16 GLM is compliant with navigation requirements.

### INTRODUCTION

The Geostationary Operational Environmental Satellite-R Series (GOES-R) is the next generation of geostationary weather satellites for the United States [1]. The first of this series was launched on November 19, was renamed “GOES-16” upon reaching geostationary orbit, and was designated “GOES-East” upon reaching its operational position over the western Atlantic. The primary optical payload on GOES-16 is the Advanced Baseline Imager (ABI), a scanning multispectral imaging radiometer [2]. GOES-16 also includes a newly-developed instrument, the Geostationary Lightning Mapper (GLM). The first operational lightning mapper flown in geostationary orbit, GLM measures total lightning activity continuously over the Americas and adjacent ocean regions, enabling forecasters to focus on developing severe storms much earlier, before they produce damaging winds, hail, or tornadoes [3]. The GLM level 1B product is near real-time optical lightning events that have been calibrated, navigated, and time tagged. GLM also generates regular snapshot “background images” of its field of view. These background images are not a formal product and thus do not have formal navigation requirements. However, they are navigated with the same algorithm as the lightning events, and thus the navigation performance (NAV) of the background images can be considered a proxy for the NAV accuracy of the lightning events [4]. The GOES flight project performs independent assessments of the GLM Image Navigation and Registration (INR) performance by evaluating the background images with the INR Performance Assessment Tool Set (IPATS) [5]. The GLM background images have several unique features that lead to non-standard image processing and INR evaluation, as described further herein.

### IPATS OVERVIEW

IPATS, developed by the GOES-R Flight Project to facilitate evaluation of INR performance of ABI and GLM, is comprised of two distinct tools, the Image Pair Selector and Evaluator (IPSE) and the Output Database Analysis Tool (ODAT). IPSE determines the misregistration in pixels between two input images, and can draw on a variety of image correlation algorithms and pre-processing optimizations. ODAT is used to process the IPSE output, perform post-processing optimizations, and generate reports and visualizations of IPSE results. More detail is provided in [5], and the registration evaluation process is described qualitatively in Figure 1.

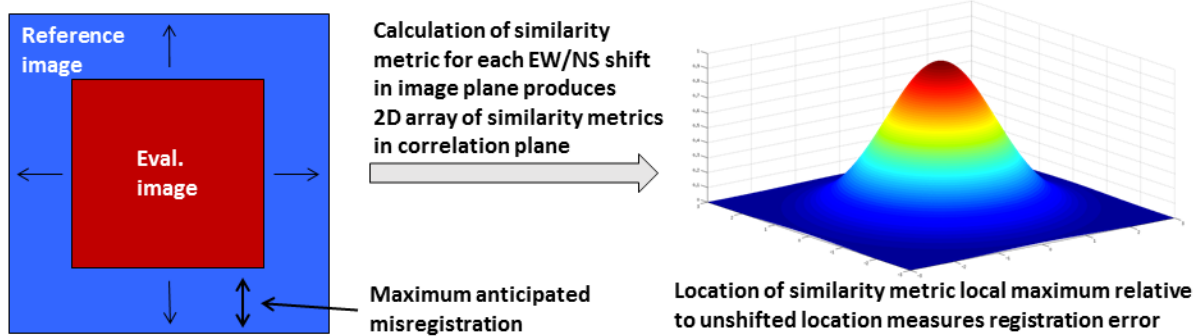


**Figure 1:** Cross correlation approach to INR evaluation using image registration. The evaluation image is shifted within the reference image, and the misregistration is determined from the offset between the similarity metric maximum and the unshifted location. Modified from [5].

For relative assessments, images are compared to other images of the same type (e.g., ABI image to ABI image). Relative assessments of ABI imagery include frame-to-frame registration (FFR), in which adjacent temporal collects are compared, and band-to-band registration (BBR), in which different bands of a single ABI scan are compared. For absolute assessments (ABI NAV), images are compared to truth images (Landsat-based image “chips”) [5].

### GLM NAV with IPATS

For GLM navigation assessment, IPATS computes the misregistration between navigated background images and the temporally-closest well-calibrated and navigated ABI level-1B full disk imagery from band 3 (0.86  $\mu\text{m}$ , 28  $\mu\text{rad}/\text{pixel}$ ), which has been found to offer the best performance as a reference band. IPSE includes several GLM-specific pre-processing optimization options, including a user-definable threshold for temporal offset between ABI and GLM images, based on the start time of the ABI image acquisition and the acquisition time of the GLM image. If no ABI image is found that satisfies this temporal offset threshold, evaluation of the GLM background image is skipped. Note that temporal mismatches between ABI and GLM images is a significant potential error source in GLM NAV analyses, especially as the temporal offset is spatially variable within the image. This variable offset is due to fundamental differences between the scanning ABI and staring GLM sensors; ABI scans require several minutes to acquire the full disk (exact timeline dependent on ABI mode), whereas GLM background images are snapshots (captured near-instantaneously) [4, 6].

### GLM Background Image Resampling

Wide field-of-view staring sensors at geostationary altitudes would typically suffer from significant extreme parallax effects that substantially degrade spatial resolution at large off-nadir angles. GLM has a novel design to mitigate these effects using a non-traditional irregular focal plane pitch (pixel size) [3]. While typical geostationary imagers, including ABI, collect data that is regularly sampled in angular (fixed grid) space [6], the GLM background images (after downsampling by the GOES ground system) have non-uniform angular spacing because of the unusual focal plane design [4]. This irregular pixel size violates a key assumption of modern digital image processing techniques, that pixels are arranged on a regular grid. To account for this, IPSE includes a bespoke irregular image resampler, which resamples the irregularly-spaced GLM images to a regular “ABI-like” angular grid and enables the GLM background images to be treated as if they were sampled to a regular grid. The current baseline configuration resamples both ABI and GLM images to an intermediate resolution of 56  $\mu\text{rad}/\text{pixel}$ . The irregular grid resampling algorithm is illustrated conceptually in Figure 2.

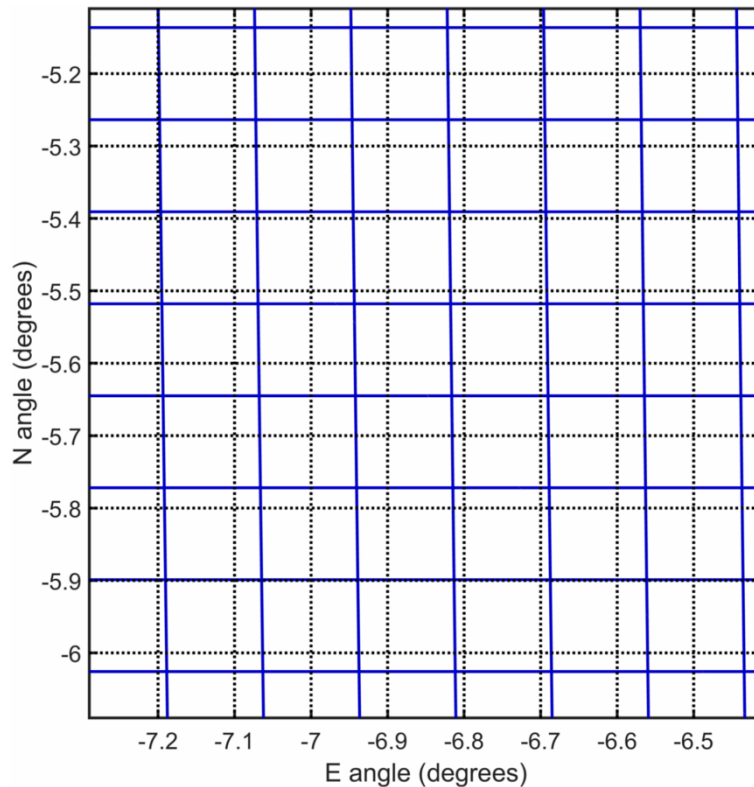


**Figure 2:** Conceptual illustration of GLM irregular angle resampler algorithm. The solid blue lines indicate the angular coordinates of the GLM pixels (lines are plotted every 10 pixels), and the regular “ABI-like” grid is shown in dotted black lines. The irregular nature of the GLM grid is demonstrated by the spatially-variable misalignment between the solid and dotted lines. A small subset of a full GLM background image is illustrated, with grid resolution reduced for clarity. A local search algorithm is employed to assign GLM pixel values to resampled “ABI-like” pixels.

### **GLM NAV evaluation locations**

IPATS performs correlation analyses at a series of geographic locations defined a priori. For ABI NAV, these locations are defined by the locations of the Landsat-based truth image chips. For all other evaluation modes, the locations, referred to as “windows” are defined by the IPSE input location database file. The master location database file includes windows placed at the geographic location of the Landsat-based truth images used for ABI NAV evaluations, as well as a series of windows placed in a regular grid across the full disk. These windows can be enabled or disabled for specific evaluation types. For example, in the case of FFR, windows over oceans are disabled because the temporal offset between ABI frames (at least 5 minutes) allows for significant cloud motion between images and clouds are the dominant signal over oceans. However, such windows are more useful for BBR evaluations since the bands within an image are captured simultaneously (indeed, as some bands do not “see to ground”, clouds are often the only feature on which cross-band registration can be based in some cases). For GLM NAV, windows are excluded from analysis if their center is over water, as the dominant error in such locations tends to be driven by cloud motion, similar to FFR evaluations. Windows are also excluded if they are close to the edge of either the earth limb or of the GLM field of regard. The set of evaluation locations used for GLM NAV analyses at the checkout orbit of 89.5° W is illustrated in Figure 3.

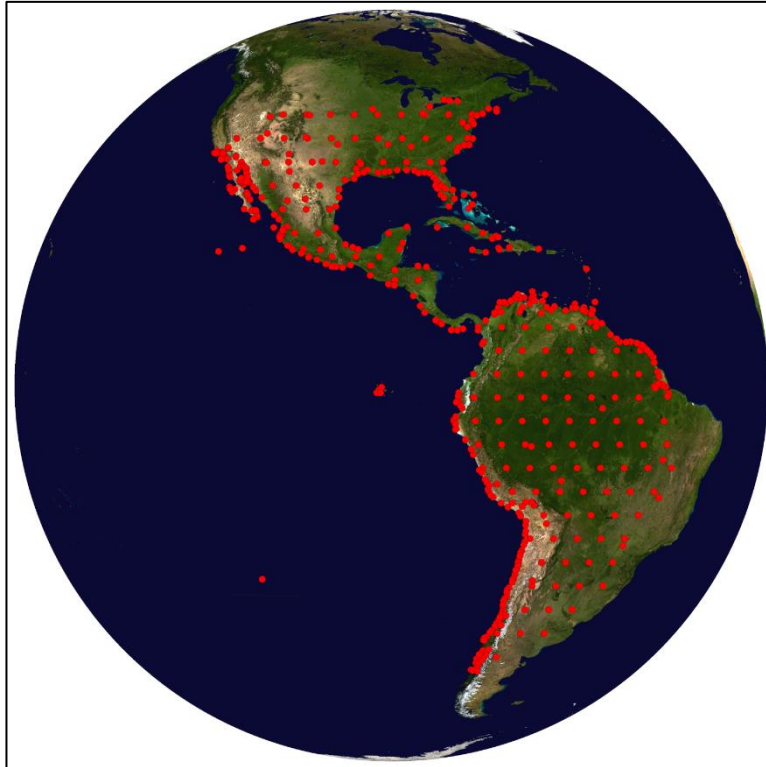


**Figure 3:** Illustration of GLM evaluation locations for the 89.5° W longitude checkout orbit. Points illustrate the centers of the evaluation location “windows”. Locations are defined based on the locations of the Landsat chip truth images used for ABI NAV evaluations plus a set of regular grid locations. Windows near the edge of the limb of GLM field of view are excluded and not shown in this figure. Background image source: NASA.

### **QUALITY FILTERING OF IPATS RESULTS**

IPATS evaluates INR performance for an image by statistically evaluating a set of localized correlations (IPSE results for individual evaluation windows). That said, many of the local correlations suffer from reduced accuracy for a variety of reasons (clouds/cloud motion, illumination conditions, scene content differences from truth image, errors in the correlation process, etc.). Judicious filtering of results to exclude such correlations dramatically improves the INR assessment. Appropriate quality filtering is particularly important for GLM NAV because of the temporal offset between a GLM background image and the temporally-closest ABI image (cloud motion, even variably within an individual image, is a major concern). Significant effort has been expended to optimize this post-processing filtering for GLM NAV.

The primary parameters used to perform quality filtering for GLM NAV are analytic measurement uncertainty (AMU), solar zenith angle (reject low sun angles), extreme outlier rejection using the median absolute deviation (MAD), and the “clear sky ratio” (CSR; fraction of clear to cloudy pixels based on the ABI clear sky mask product). The progressive application of these filters is illustrated in Figure 4. AMU is a mathematical construct that parameterizes the level of false misregistration derived, for images that are perfectly navigated and registered, resulting from “noise” sources such as variation in illumination conditions, scene content differences, and error in the correlation process. AMU incorporates image contrast, image size (number of pixels) and the typical magnitude of image perturbations not associated with image translations. For more detail, please see [5].

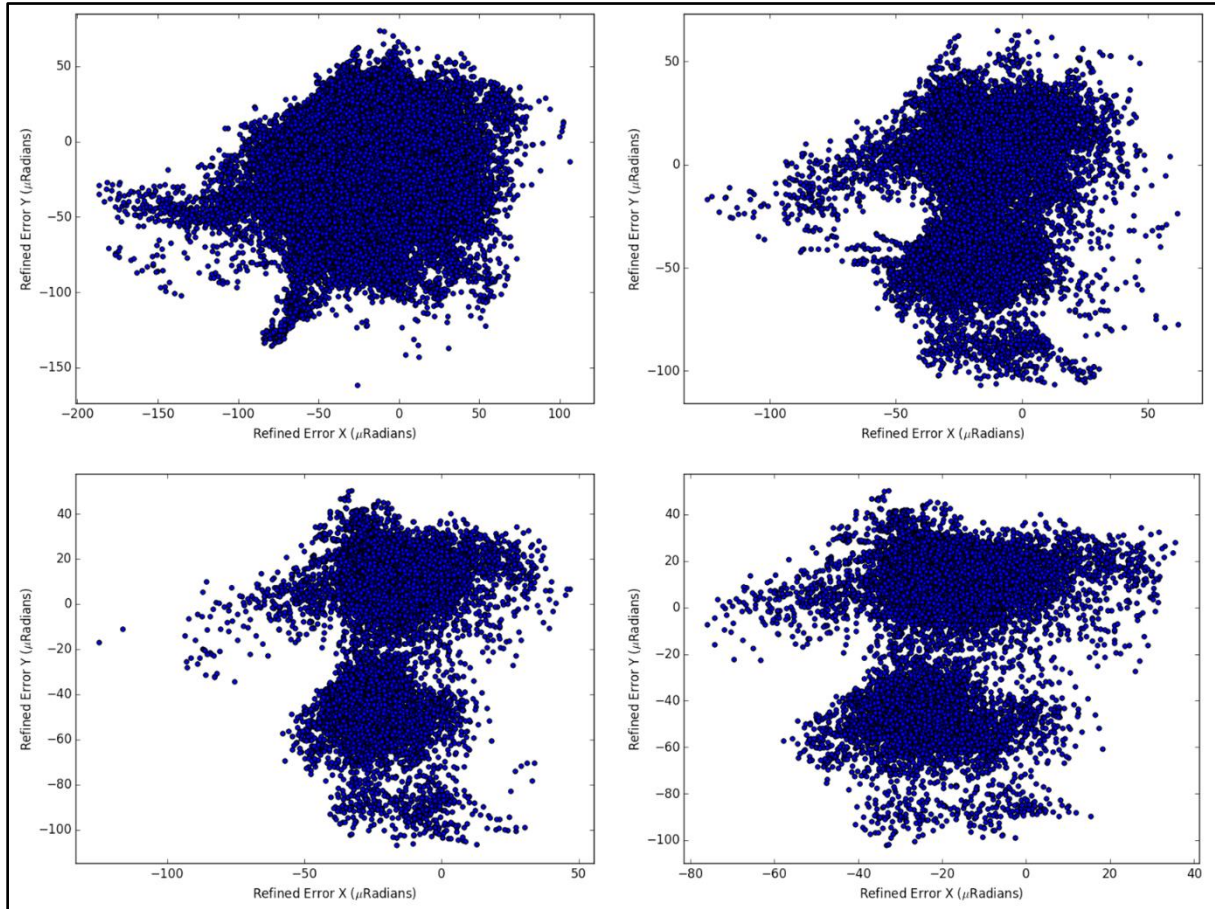


**Figure 4: Progressive application of quality filtering thresholds to the filter training dataset. Plots show Y (NS) error vs. X (EW) error in microradians ( $\mu\text{rad}$ ). Upper left:  $\text{SZA} < 75^\circ$ ; Upper right:  $\text{AMU} < 2.52 \mu\text{rad}$ ; Lower left:  $\text{CSR} > 250$  (25%); Lower right:  $9^\circ\text{MAD}$  extreme outlier rejection. The bimodal N/S behavior is an artifact of a GLM focal plane anomaly and is addressed via hemispheric stratification of results.**

GLM NAV is a relative assessment (there is no absolute truth reference), so the INR performance is assessed primarily through statistical assessments like dispersion (standard deviation) and stability. Filtering thresholds are evaluated by trading reduced dispersion against maintaining sufficient sample size for reliable statistics. Baseline quality filtering thresholds were selected from analysis of multiple full days of GLM background images collected in the fall of 2017. The filtering configuration illustrated in Figure 4 is considered the baseline configuration for processing other GLM background image datasets. The thresholds are revisited on an as-needed basis to ensure that they are tuned appropriately for analysis of newer background images.

## IPATS GLM NAV EXAMPLE RESULTS

Results for two datasets collected in fall of 2017 are presented below in Table 1, in the form of mean values compiled across the full multi-day span of each dataset, and stratified by hemisphere in each case. The 28 Sep 2017 set is the quality filter “training set”, and the post-filtering results are illustrated in Figure 4 (lower right). The 31 Oct 2017 set was evaluated using the filtering thresholds derived from the 28 Sep 2017 (training) set. Systematic NAV error between N and S hemispheres is a known artifact that is not currently addressed by the GLM NAV algorithm.

	28 Sep 2017 N Hem	31 Oct 2017 N Hem	28 Sep 2017 S Hem	31 Oct 2017 S Hem
$\sigma_x$	11.2	10.0	11.3	12.1
$\sigma_y$	9.5	9.5	15.4	14.3
Mean X	-18.1	-14.0	-22.4	-27.2
Mean Y	12.7	11.4	-49.8	-54.1
$ \bar{X}  + 3\sigma_x$	51.8	44.2	56.4	63.5
$ \bar{Y}  + 3\sigma_y$	41.2	39.8	96.0	96.9
n	15420	10322	5764	2062
# images	186	166	175	141

**Table 1:** GLM NAV results for two datasets collected in fall 2017, stratified by hemisphere. Positive error indicates the image is shifted to the east (EW) or north (NS) with respect to the reference/truth image.

The 28 Sep 2017 set results summarized in Table 1 are illustrated graphically in Figure 5, which illustrates per-image temporal trends in estimated navigation error and sample size.

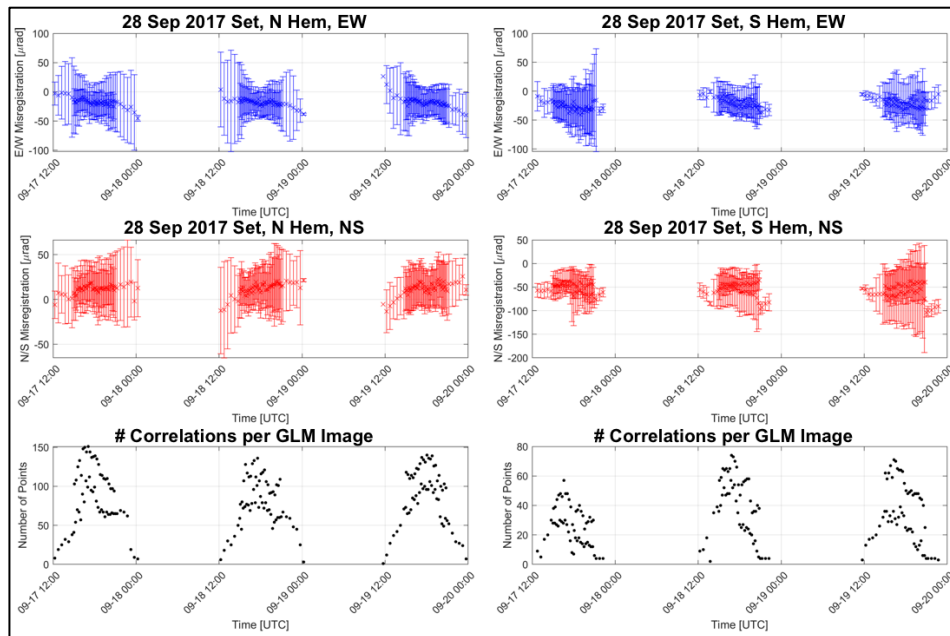


**Figure 5:** GLM NAV results for 3 days of GLM background images from September 2017. Quality filtering has been applied as described above. Results are shown as a function of GLM background image acquisition time, on a per-image basis. EW error is shown in the top (blue) plot, NS error in the middle (red) plot, and number of correlations contributing to the error estimate for each image in the bottom (black) plot. Error bars on the EW and NS plots are  $\pm 3\sigma$ .

## DISCUSSION

While the number of individual correlations (n) is smaller in the 31 Oct 2017 results as compared to the 28 Sep 2017 results, in both cases the metric of mean X or Y error plus  $3\sigma$  are mostly on the order of 40-60  $\mu\text{rad}$ . The exception is the Y (north-south) error in the southern hemisphere, where this error “metric” approaches 100  $\mu\text{rad}$ . Recall that IPATS is the GOES-R Flight Project’s tool for performing independent evaluation of NAV performance. Note that while IPATS results are suggestive of the formal GLM NAV performance, the IPATS assessment is not a formal validation of GLM NAV accuracy against the L1B event navigation requirement. In both datasets presented above (Table 1, Figure 5), results suggest compliance with the GLM NAV requirement of 112  $\mu\text{rad}$  navigation accuracy for the lightning events [7]. The 31 Oct 2017 set has a smaller number of correlations remaining after filtering. This is likely due to increased cloud cover over a few key areas of the disk during those collections, although sample size issues are the subject of ongoing research. Sample size roughly follows the expected trend with time of day, with maxima near local noon (Figure 5, bottom). The

somewhat irregular nature of this correlation is likely due to the discrete spatial sampling of the disk (Figure 3) and variable temporal offset between the ABI and GLM images.

## **SUMMARY/CONCLUSIONS**

We have demonstrated functional, quantitative assessment of the navigation accuracy of GLM background images using IPATS. In the process, we have defined a set of post-processing quality filtering thresholds that are effective at clarifying INR performance. Independent (though informal) GLM NAV evaluation with IPATS has been demonstrated. The filtered results for the GLM background image datasets evaluated herein suggest that GLM is compliant with its level 1B navigation requirements.

## **REFERENCES**

1. A. Krimchansky, D. Machi, S. A. Cauffman, and M. A. Davis, "Next-generation Geostationary Operational Environmental Satellite (GOES-R series): a space segment overview," in *Remote Sensing*, 2004, vol. **5570**, p. 10: SPIE.
2. T. J. Schmit, M. M. Gunshor, W. P. Menzel, J. J. Gurka, J. Li, and A. S. Bachmeier, "Introducing the Next-Generation Advanced Baseline Imager on GOES-R," *Bulletin of the American Meteorological Society*, vol. **86**, no. 8, pp. 1079-1096, 2005.
3. S. J. Goodman et al., "The GOES-R geostationary lightning mapper (GLM)," *Atmospheric Research*, vol. **125**, pp. 34-49, 2013.
4. Lockheed Martin Space Systems Company, "Navigation Design Document [CDRL 046], Revision D," Advanced Technology Center - Cage Code 651132014.
5. F. J. De Luccia et al., "Image navigation and registration performance assessment tool set for the GOES-R Advanced Baseline Imager and Geostationary Lightning Mapper," in *Earth Observing Missions and Sensors: Development, Implementation, and Characterization IV*, New Delhi, India, 2016, vol. **9881**, pp. 988119-988119-17: SPIE.
6. Harris Corporation, "Product Definition and Users' Guide (PUG) Volume 3: Level 1B Products for Geostationary Operational Environmental Satellite R Series (GOES-R) Core Ground Segment, Revision 1.1, October 2017, <http://www.goes-r.gov/users/docs/PUG-L1b-vol3.pdf>," Melbourne, FL2017.
7. GOES-R Flight Project/Code 417, "GOES-R Series Geostationary Lightning Mapper (GLM) Performance and Operational Requirements Document (PORD)," NASA GSFC2012.